

Magnetohydrodynamics Generator with Plasma Layers as Power Source Aboard a Hypersonic Airplane

Vadim S. Slavin,* Valery M. Gavrilov,† Nikolay I. Zelinsky,† and Alexandr R. Bozhkov†
Krasnoyarsk State Technical University, 660074, Krasnoyarsk, Russia

The application of a magnetohydrodynamic (MHD) generator as a power source on a hypersonic airplane is analyzed. A new type of an MHD generator is considered, using nonuniform gas–plasma flows, where production of plasma pistons (T-layers) is realized by special provoking of an overheating instability. This process is initiated in cold air, transforming the kinetic energy of the incoming airflow directly into electric energy without further heat addition or seed injection. Calculations show that, in flight at $M \approx 7$ and at an altitude of 30 km, the rate of power transformation will be approximately 30%, the optimal value of magnetic field being $B \approx 0.3$ T. An experiment to investigate the stability of a plasma piston interacting with the air stream and magnetic field has been carried out. A shock tube facility was used to create conditions corresponding to those of an MHD generator on a hypersonic airplane. A plasma layer was established within the MHD channel (~ 1.5 m length), and its parameters agreed with calculations based on a piston model. A nonstationary quasi-one-dimensional computing program was used to simulate the experimental conditions. Because of energy expenses on gasdynamic dilatation and ionization of air and radiation, heat input into a discharge is nearly twice as large as the internal energy of the working medium.

Nomenclature

A	=	cross section of channel
a	=	width of electrodes
B	=	magnetic induction
C	=	capacity
E	=	electromotive force
E_y	=	electric field
e	=	total specific energy of gas
h	=	height of magnetohydrodynamics(MHD) channel
I	=	current in load
j	=	current density in plasma
K	=	load factor
L	=	inductance of load
M	=	mach number
M_0	=	mach number at inlet of MHD channel
P	=	static pressure
P_s	=	stagnation pressure of isentropy flow
P_0	=	static pressure at inlet of MHD channel
Q_j	=	energy discharge in plasma by joule heating
Q_r	=	energy extraction from plasma with radiation losses
q	=	electric charge of capacity
q_r	=	power of specific radiation losses
R	=	resistance of load
R_p	=	resistance of plasma
S_r	=	flux of radiation energy
T	=	static temperature
T_s	=	stagnation temperature of isentropy flow
T_0	=	static temperature at inlet of MHD channel
t	=	time of process
u	=	velocity of gas flow
V	=	voltage on capacity
W	=	electric power of MHD generator
x	=	coordinate along the MHD channel

ΔP	=	overfall of pressure on the T-layer
ΔV	=	near-electrode voltage drop
δ	=	thickness of T-layer along x direction
ε	=	internal specific energy of gas
ε_p	=	total internal energy of T-layer
ε_r	=	coefficient of radiation emitted by a semisphere plasma volume
ρ	=	mass density
σ	=	conductivity of plasma
σ_r	=	Stefan–Boltzman’s constant

Introduction

A MAGNETOHYDRODYNAMICS (MHD) generator using a uniform flow of combustion products as a working medium has a number of problems for open cycle MHD programs. These features are low electric conductivity of gas with alkali seed at a temperature of $T \approx 3000$ K, which becomes lower with the expansion of gas in the channel and the requirement for strong magnetic fields, which leads to the necessity of superconductive magnetic systems.

Application of a nonuniform working medium, where different temperature zones will be generated, resolves some of these problems. Separation of working functions between flow zones with different temperatures will occur here. The main part of a working medium in the nonconductive sections of the flow expands adiabatically, pushing electric conductive clots in a cross magnetic field; their enthalpy minus joule dissipation is released in the hot clots being converted into electric energy. A smaller part of the working medium is contained in electric conductive layers through which all of the electric current flows and which play the role of plasma armature in an electric power MHD generator. At sufficient current density, the plasma current layers assume a self-sustained mode. As a result, high MHD process efficiency can be obtained even though the mass average temperature of the whole flow is low.

The one-dimensional analysis¹ showed that the temperature for thermal stabilization of plasma in the current layers is about 10^4 K. Under such conditions, high electric conductivity is achieved without alkali seed. These calculations showed that it is possible to ensure an effective generator process at sufficiently low values of magnetic fields and to use the impulse nature of the electric current on the load for direct generation of alternating electric current.

Received 9 March 1999; revision received 5 August 1999; accepted for publication 5 November 1999. Copyright © 2000 by the authors. Published by the American Institute of Aeronautics and Astronautics, Inc., with permission.

* Professor, Head, Magnetohydrodynamics Works, 26 Kirensky Street. Krasnoyarsk, 660074, Russia; Fax: (3912) 43-06-92.

† Associate Professor, Magnetohydrodynamics Works.

Investigations of MHD processes in nonuniform gas-plasma flows were begun in the middle of the 1960s (Ref. 2). The pioneer works revealed the possibility of operating an MHD generator with a nonuniform working medium and, on the basis of linear analysis of the development of instability on the separation surface of the gas and plasma, showed that the instability would destroy the current layers structure. In many respects, due to these results, interest in the application of nonuniform flows has been lost for almost 30 years, and investigations of one of the possible types of nonuniform flows, the so-called gas-plasma flows with T-layers, were continued only in Russia.

The discovery of the T-layer as a physical phenomenon³ was made as a result of numerical simulation of the process with strong MHD interaction of plasma flow with a magnetic field. Essentially, the T-layer is a nonlinear phase of development of the overheating instability where the temperature nonuniformity creates an electric conductivity channel for the Faraday current. The T-layer is stabilized at $\approx 10^4$ K by the radiation losses. The spontaneous creation of the T-layer was revealed in an experiment⁴ and was proved in a numerical simulation of this experiment.⁵ Because the experiment had not revealed any effects of instability of the gas and plasma separation surface, it was decided to investigate the possibility of the creation of an MHD generator with nonuniform gas-plasma flow based on the T-layer phenomenon.⁶ However, as further numerical simulation⁷ showed, there appeared great difficulties in using the T-layer concept to create a high-power (more than 200 MW) open cycle generator. One of the difficulties was the very high radiation losses from plasma of combustion products, which cause all of the current in the MHD channel to be collected in a single current layer. In this case, powerful shock waves inevitably arise, sufficiently decreasing isentropic efficiency. The second difficulty was that the current layer thickness does not exceed 3–5 cm, which makes doubtful the possibility of overlapping the cross section of a real MHD generator with such a thin plasma piston.

This result led to another solution,⁸ the essence of which is in using large-size temperature nonuniformities in a flow containing alkali seed.

Nevertheless, one can point out two fields of application where the MHD-generator with unseeded current layers might work efficiently. The first is an MHD generator on a hypersonic airplane, which transforms part of the kinetic energy of the airflow into electric energy.^{9,10} The second application is a closed-cycle MHD generator operating with nonequilibrium current layers in a noble gas flow. The idea of MHD generator with nonequilibrium current layers has been investigated in the work,¹¹ where possible types of instabilities in nonuniform and nonequilibrium argon plasma are analyzed. The possibility of organization of stratified flow is shown and the concept of an MHD generator with a Faraday-type channel is formed.

The aim of this work is the analysis of the possibility of creating the first type of MHD generator, that is, an electric power generator on a hypersonic airplane. The T-layer MHD generator experiment was carried out to access the use of unseeded air as the working medium. Additional computer simulations were carried out to help understand the test results.

Airborne MHD Generator for a Hypersonic Airplane

The main problem of application of MHD generators onboard an airplane is the bulky and heavy magnetic systems. The traditional MHD method of energy conversion deals with very low efficient electric conductivity of a uniform flow of a working medium. To adjust this drawback according to the formula for specific power of an MHD generator

$$w = \sigma K (1 - K) u^2 B^2 \quad (1)$$

it is necessary to increase the magnetic field. The required value ($B \approx 4$ T) is realized with superconducting electromagnets, whose weight and size characteristics are not suitable for airplane conditions.

In an MHD generator with T-layers, a nonuniform flow is formed where T-layers occupy no more than 10% of the MHD channel volume. Plasma electric conductivity in these current layers are in excess of 10^3 S/m, and under these conditions the average electric conductivity of the whole nonuniform flow is considerably higher than that for a uniform flow case. Therefore, it is possible to lower the magnetic field to ≤ 1 T, which can be realized by means of permanent magnets.

An MHD generator on a hypersonic airplane converting the kinetic energy of the air stream into electric energy will not have very strict requirements on the isentropic efficiency of the process. Hence, one can reduce the load factor and maximize the specific power in the MHD channel, that is, to work with $K = 0.5$. Lowering the load factor K lead to increasing joule heating. It allows us to support the T-layer at a lower MHD interaction. Thus, the negative effect from the strong shock waves can be decreased. Finally, working with air and not with combustion products reduces radiation losses that change the structure of the T-layer. It becomes thicker and accordingly more stable. Thus, it should be acknowledged that the conclusion that an MHD generator with T-layers for work in an open cycle is useless⁷ has proven to be wrong for hypersonic airplane conditions. It will probably turn out to be the most efficient facility as an airborne source of electric energy.

Consider an unsteady one-dimensional process in the MHD channel shown in Fig. 1. Here an input device accomplishes deceleration of the airflow from $M_{\text{flight}} = 7$ to $M \approx 3$. The decelerated flow enters into a rectangular channel with short electrode inserts in the narrowest part connected to the external system of the periodic impulse discharge. The discharge forms a plasmoid in the airflow that is picked up by the flow and injected into the MHD channel with the cross magnetic field. The electrode walls of the channel are segmented. The first pair of electrodes is a short circuit, and the load on the following ones is selected so that it satisfies the condition $K = E_y (u \times B) = 0.5$. A short-circuit section is required for the production of a T-layer structure from a plasmoid, which means that there are two balances, force balance

$$\Delta P = B \int_{\delta} j \, dx \quad (2)$$

and energy balance

$$j^2 / \sigma = \text{div} S_r \quad (3)$$

performed on this T-layer.

The system of impulse discharge works at a set frequency and transforms the airflow into a stratified structure where the T-layers interact with each other through gasdynamic disturbances. Extreme disturbances can break down the condition of balances (2) and (3) for the following T-layers resulting in their disintegration and the lack of formation of a periodic structure. The aim of this numerical simulation is the demonstration of a generator mode where the efficiently working periodic structure of T-layers is being formed.

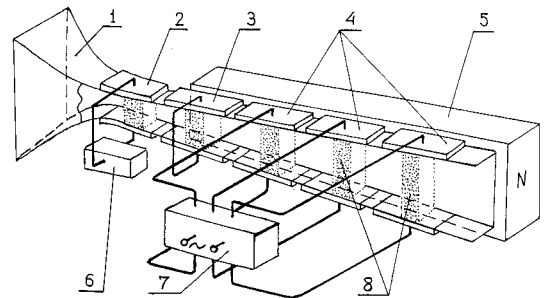


Fig. 1 Hypersonic plane MHD generator concept scheme: 1) oncoming air stagnating input device; 2) plasma clots initiating section electrode; 3) T-layer forming section electrode; 4) working section electrodes; 5) permanent magnet element; 6) initiating section periodical impulse discharge supplying system; 7) alternating current load supplying adjustment interface; and 8) plasma clots (T-layers).

Table 1 Parameters of the simulated airborne MHD generator

Parameter	Value
Static pressure in oncoming flow	10^3 Pa
Outside air temperature	240 K
Flight speed	2135 m/s
Pressure in channel throat ($M_0 = 3$)	1.13×10^5 Pa
Temperature in channel throat	925 K
Air speed in channel throat	1796 m/s
Throat cross section	57×10^{-4} m ²
Electrodes width	0.1 m
Channel height in the throat	0.057 m
Channel height at the exit	1 m
Plasmoid initial temperature	7×10^3 K
Plasmoid initial thickness	0.05 m
MHD channel length	6 m
Load factor	0.5

Assume that the flight is performed at an altitude of 30 km at a velocity of $M_{\text{flight}} = 7$ and that flow deceleration to $M_0 = 3$ occurs isentropically. The flow and MHD generator parameters are given in Table 1. The value of the magnetic field should be selected to find the optimal mode.

Mathematical Model

The process is described by the system of quasi-one-dimensional MHD equations:

$$\frac{\partial \rho A}{\partial t} + \frac{\partial \rho u A}{\partial x} = 0 \quad (4)$$

$$\frac{\partial \rho u A}{\partial t} + \frac{\partial [(\rho u^2 + P)A]}{\partial x} - P \frac{\partial A}{\partial x} = jBA \quad (5)$$

$$\frac{\partial \rho e A}{\partial t} + \frac{\partial [\rho u A(e + P/\rho)A]}{\partial x} = (jE - q_r)A \quad (6)$$

where $e = \varepsilon + u^2/2$ is the complete gas energy.

For the current density and the electric field, the following equations are used:

$$j = \sigma(E - uB), \quad E = KuB \quad (7)$$

Equation system (4–6) is complemented by thermodynamic relationships for pressure $P(\rho, \varepsilon)$ and temperature $T(\rho, \varepsilon)$ given in the tables of Ref. 12 and electric conductivity dependence on T , $P - \sigma(T, P)$ (Ref. 13). Volume radiation losses for air can be estimated by a model of a volume radiator

$$q_r = 4\sigma_r T^4 \left[\frac{\varepsilon_r(P, T, x - x_1)}{2(x - x_1)} + \frac{\varepsilon_r(P, T, x_2 - x)}{2(x_2 - x)} \right] \quad (8)$$

where $\sigma_r = 5.67 \times 10^{-8}$ W/m² · K⁴; $x_1 \leq x \leq x_2$, where x_1 and x_2 are distances from the calculated point up to the upstream and downstream boundaries of a T-layer, correspondingly; and $\varepsilon_r(P, T, l)$ is emission ability of hemispheric isothermal volume with radius l (Ref. 14). Relationship (8) was compared with a more detailed calculation¹⁵ for a nonisothermal layer of air plasma. In a wide range of changes, P , T , and l deviation did not exceed 50%.

The boundary conditions of the problem are determined by its formulation: At the MHD channel inlet (cross section $x = 0$) steady-state conditions with the parameters $P_0 = 1.13 \times 10^5$ Pa, $T_0 = 925$ K, and $u_0 = 1796$ m/s are set. At the channel exit ($x = 6$ m) the flow has a pulsating nature, but still remains supersonic, which enables the prescription of conditions $\partial f / \partial x = 0$. Steady isentropic flow is the initial condition of the problem.

For the numerical solution of the equation set (4–6), a two-step difference Lax–Vendroff scheme is used, modified by means of the local dissipation method.¹⁶

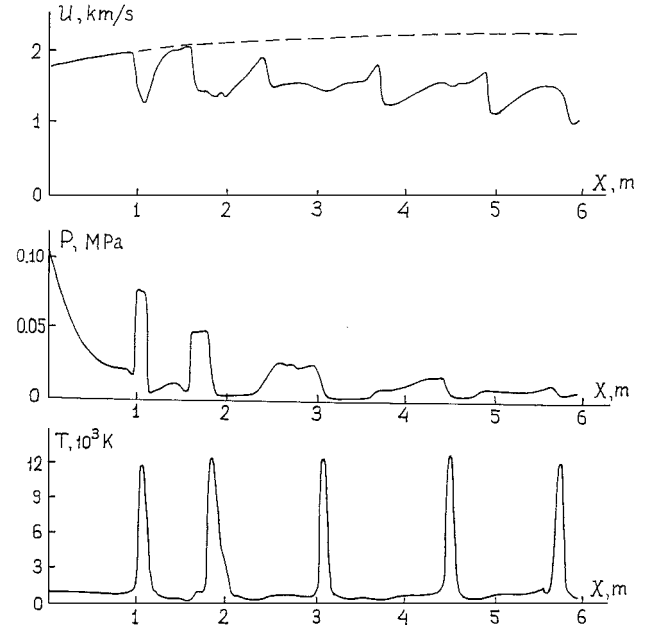


Fig. 2 Nonuniform gas-plasma flow velocity, pressure and temperature distributions. The curves correspond to the moment after establishing the periodical mode.

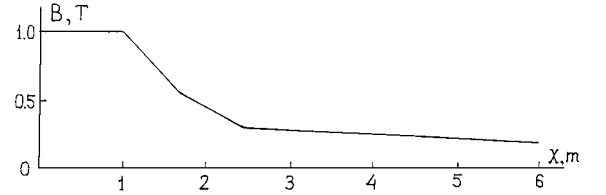


Fig. 3 The MHD channel magnetic field distribution. The field is created by the permanent magnet system.

Simulation Results

Figure 2 shows the distribution of velocity, pressure, and temperature in the MHD generator channel at one of the moments of the steady-state periodic process. Steady distribution of the magnetic field (shown in Fig. 3) corresponds to the given mode. At this moment of time, there are five current layers [see relationship $T(x)$] in the MHD generator channel, and their maximum temperature reaches 12×10^3 K. The current layers actively interact with the flow, which results in the appearance of shock waves and expansion waves. These waves can be identified on the curves $P(x)$ and $u(x)$, the gradient zones with $\partial P / \partial x > 0$ corresponding to the fronts of shock waves, and the zones with $\partial P / \partial x < 0$ being current layers where pressure drop is balanced by electrodynamic force.

The development of T-layers includes the following two stages.

The first stage is the pick up of the temperature disturbance set in the inlet of MHD channel. In the unseeded airflow at the initial temperature about 7000 K, the disturbance has low electric conductivity and is moved by the flow practically without force interaction. However, in the short-circuit section of the channel, the joule heating of the plasma exceeds the cooling one because of the flow expansion. Then the mechanism of overheating instability turns on; after which a plasma clot develops like an explosion. Pressure in a T-layer does not have time to level off and, as seen on the graph $P(x)$ for current layer turned out in the cross-section $x = 1$ m, the pressure peak corresponds to the thermal spike. The temperature of the T-layer at that time reaches 12×10^3 K and its further elevation is decelerated by radiation energy losses.

The second is the working stage. The T-layer is thermally stabilized by radiation losses, and its temperature does not rise. The pressure peak decays and the pressure gradient balances the electrodynamic force. At this stage the flow influences on a T-layer as on

a plasma piston. The part of this work is released in the load, and the remaining part maintains the self-support mode of the T-layer; it manifests itself as joule dissipation.

As the T-layer travels along the channel, the gas pressure is permanently dropping, and hence, the power of the radiation losses is also dropping. Limitation of undesirable temperature increase is attained by decreasing the magnetic field along the channel. The efficient periodic mode, which is operating with five current layers in the working section of the MHD channel, is supported by a magnetic field with an average value of $\langle B \rangle = 0.3$ T. Such a field is easily created by permanent magnets.

In the numerical simulation process, the electric power of an MHD generator was determined as $W = 3$ MW in the periodic mode. Expenses for the generator's own needs, that is, for initiating current layers, are $W_{\text{own}} = 0.5$ MW in this mode. This is net expenditure, ignoring losses that in real discharge systems could make the expenditure approximately above 50% higher. However, even in this case there remains a considerable store of useful power, which makes the idea of the MHD generator with T-layers attractive for the given application.

Experimental Investigation of T-Layer in the Airflow on a MHD Shock Tube

In the preceding section the results of a mathematical simulation of the processes in nonuniform gas-plasma airflow in the channel of the MHD generator operating onboard a hypersonic airplane were presented. A one-dimensional model was used, assuming one can maintain the quality of a piston structure of current layers but, as it was noted in the Introduction, it is just that which gives rise to doubt. At the boundary of the conducting and nonconducting mediums, wavelike disturbances can appear under the influence of electrodynamical force. They arise in the form of cold jets. Development of this instability, known as the Rayleigh–Taylor instability, can lead to the decay of the current layer into separate current channels flowing around with the gas flow. If the basic mechanism of energy losses for a uniform plasma piston are radiative, then for a T-layer decayed into separate arcs, convective heat exchange with carrier gas flow will prevail. The change of energy balance of an electric arc results in the change of its volt-ampere characteristic that for a T-layer, which is the arc itself supported by the source with the constant electromotive force (uBh), will lead to its extinction.

A typical time of development of the linear phase of Rayleigh–Taylor instability can be estimated by using the relationship from Ref. 17:

$$\tau_{R-T}^{-2} = n^2 = jB/(\rho\delta) \approx 10^8 \text{ s}^{-2}$$

from where it follows that $\tau_{R-T} \approx 10^{-4}$ s.

Here $j = 10^6$ A/m², $B = 1$ T, $\rho = 0.1$ kg/m³, and $\delta = 0.1$ m were taken as typical parameters. Correlation of this time with the working time of a T-layer in the MHD channel shows the inevitability of the development of instability. However, we should consider an extremely simplified approach, applied in linear analysis, that ignores both real turbulent viscosity and heat conduction. The gradient character of the boundary between the gas and plasma and the compressibility of the gas working medium are also neglected. Mathematical simulation considering all of these factors appears to be very complicated, and so to answer the question of the stability of a piston structure of a T-layer, it is desirable to carry out an experimental investigation.

An experimental facility¹⁸ was used which comprised a shock tube, supersonic nozzle, MHD channel, and vacuum tank. The shock tube is capable of achieving quasi-stationary outflow of air with a duration of about 2×10^{-3} s and with stagnation parameters of $P_s = 0.8$ MPa and $T_s = 2500$ K. The forming of the plasmoid occurs in the nozzle part of the channel. For this purpose, the divergent walls of the nozzle are made as continuous electrodes to which a battery of capacitors is connected. Electrodes of the working section of the MHD channel are separated from the nozzle electrodes by a dielectric lining. The dielectric walls of the nozzle and the working section are made of glass-reinforced plastic with optical windows that are used to observe the T-layer development. The basic dimen-

sions of the MHD channel are the following: critical cross section of the nozzle, 4×1.6 cm²; working section of the MHD channel (constant cross section), 4×8 cm²; nozzle length, 0.4 m; and length of the working section of the MHD channel, 2 m.

An external magnetic field in the volume of the MHD channel is created by Helmholtz turns, on which a condenser battery discharges. The half-cycle of a discharge was 2×10^{-2} s that enabled us to consider the magnetic field as a constant, during the T-layer motion along the MHD channel. The magnetic field value ranged from 0 to 2 T on various runs.

The process of shock start at the nozzle and the flow structure in it were investigated with the help of an interferometer-shadowgraph working together with a high-speed cine camera. The shock start time determined by the shadowgraph was 2×10^{-4} s. After the passage of the system start wave–contact surface–secondary wave, steady flow is set in the initiation section. The Mach number measurement at the MHD channel inlet was conducted using the shadowgraph picture of the flow over a half-wedge. The Mach number measured 5 cm upstream of the MHD channel inlet was $M = 2.87$.

The capacitor bank, connected to the initiation section through a spark gap, was initially charged to 5 kV. The capacity of $C = 300$ μ F was supplying a half-cycle discharge time $\approx 0.75 \times 10^{-4}$ s. The spark-gap ignition was synchronized with pressure detector signals responding to the initiation of wave input. This approach enabled the start of the initial phase of a discharge in rarefied air ($P_0 = 2$ kPa, $T = 300$ K) for which breakdown voltage < 5 kV. After passing through a discharge zone, the shock wave involved an electroconductive slab into the gas flow and the following, the basic part of a discharge passed in the flow of air just behind a shock wave. Discharge current ranged up to 20 kA, and estimating the power contribution into plasma according to the intensity of the discharge current in the modes of the short circuit and the discharge in the nozzle, one can conclude that 10–15% of the initial energy of a capacitor bank was released in the plasma during the first two half-cycles. For forming a localized plasmoid, current cutoff after the second half-cycle was envisaged. Figure 4 shows a number of successive frames of discharge development in supersonic flow from which one can see that the initiation system forms a local plasma clot.

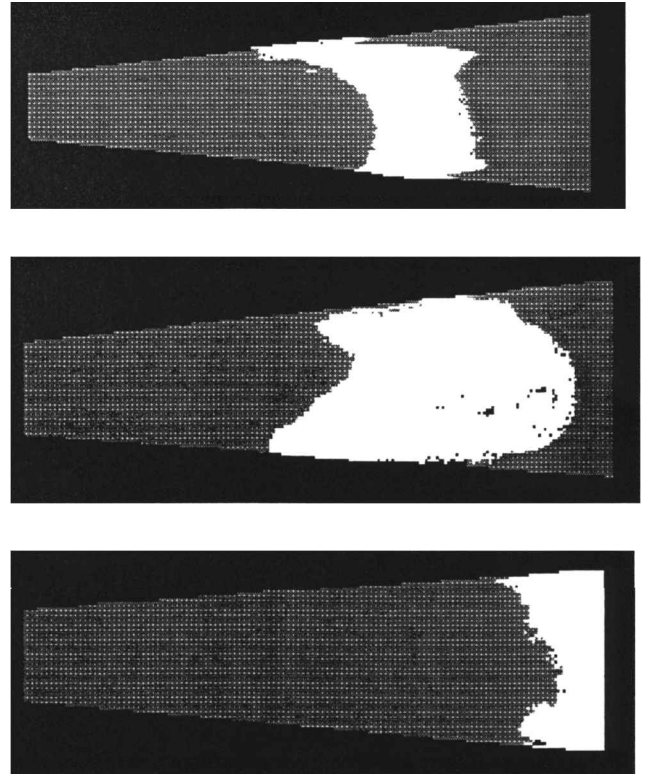


Fig. 4 Fast filming frame sequence of plasma clot discharge evolution in the initiating section.

To analyze the process in the working part of the MHD channel measurement of the total current flowing through a T-layer, the voltage across the electrodes of the MHD channel and the distribution of current density in the T-layer was envisaged. Current density was measured by current detectors, which are in fact coaxial ohmic shunts collecting current from a small section ($3 \times 40 \text{ mm}^2$), the latter one being insulated from the next electrode wall. Detectors of current density are located in five cross sections of the MHD channel with a stepsize of 250 mm.

Working the MHD channel in the generator mode in this installation is impossible because of the lack of alkali seed. Here the electric conductivity of cold near-electrode layers is actually equal to zero. Electric contact of electrodes with the plasma nucleus of a T-layer is accomplished through a system of microarcs, the junction points of which are fixed relative to the surface of electrodes, and while the T-layer is moving along the channel, the microarcs appear on its forefront and then die out on the back front. Such a description of the electrode processes is validated experimentally. After each startup of the experiment, initially cleared surfaces of the electrodes are covered with a net of pointwise spots, where both the cathode and anode are sized approximately equal. The parameters of a microarc and its voltage drop are determined by the conditions of heat exchange of the arc channel with the airflow in the boundary layer. Therefore, electrode voltage drop will appear to be constant and not dependent on the current in the T-layer, which determines only the number of microarcs. The magnetic field creates a decelerating force that must be balanced by aerodynamic resistance. An angle between the flow velocity vector in the boundary layer and the arc axis increases with an increase of the magnetic field, and as a result, the normal component of the stream velocity increases, boosting heat exchange and the voltage drop on a microarc. The experiment proved that the total voltage drop between the cathode and anode depends on a magnetic field and forms about 200–300 V. At the same time the emf in the MHD channel, where flow velocity $u \approx 1 \text{ km/s}$, $B \approx 1 \text{ T}$, and $h = 8 \times 10^{-2} \text{ m}$, is approximately 80 V. To remedy this, the bank of capacitors initially charged up to 500 V was connected to the electrodes of the MHD channel. A plasmoid closed the MHD channel electrodes, and the capacitors started to discharge. The value and direction of discharge current was set to correspond to the T-layer current under the generator mode conditions. This approach enables the compensation of near-electrode voltage drop and the realization of the MHD process corresponding to a generator mode.

In Fig. 5 one can see dependencies of current and voltage on time for modes $B = 0$ (Fig. 5a) and $B = 1 \text{ T}$ (Fig. 5b). In these modes, the configurations of the current layers were substantially different. For $B = 0$, a current layer was actually an unmodified plasmoid ($\delta \approx 15 \text{ cm}$) formed in the initiation section; for $B = 1 \text{ T}$, the MHD process of deceleration that results in substantial compression and the virtual thickness of a T-layer did not exceed 5 cm under these conditions. These experimental data were obtained in the course

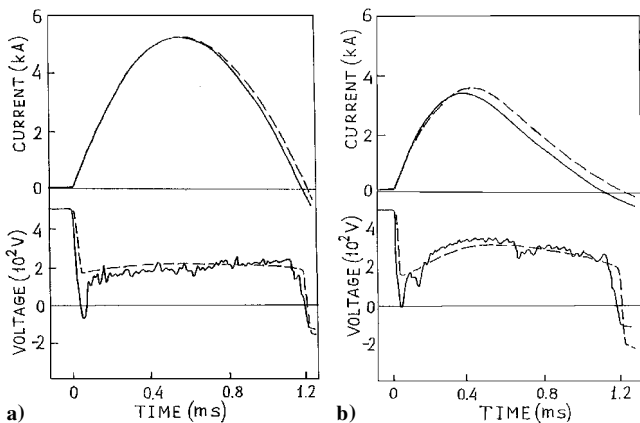


Fig. 5 MHD channel electrodes current and voltage oscillograms (solid curves correspond to experimental data, dotted lines correspond to simulation results); a-mode with $B = 0$; b-mode with $B = 1 \text{ T}$.

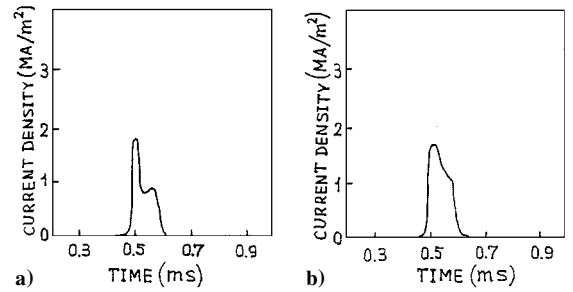


Fig. 6 Oscillogram: a) current density pick-up signal; b) obtained as a simulation result.

of processing the oscillograms from current density detectors that had fixed the shorting moment of a T-layer on a detector electrode and the time of its passage through the given cross section of the MHD channel. By comparing signals of various detectors one can determine the velocity of the T-layer motion, which is 1.4 km/s for $B = 0$ and 1 km/s for $B = 1 \text{ T}$.

These experimental data do not give any idea on the nature of interaction of a T-layer with the flow. Has the piston structure preserved its integrity or disintegrated into separate arc channels? However, it can be compared with the mathematical simulation of the same experimental mode. In this case, the numerical model of the process includes all of the effects of the external circuit, near-electrode voltage drop, and plasma processes within the one-dimensional piston description.¹⁹ The results of the numerical simulation are shown by dotted lines in Fig. 5. Good correspondence between the experiment and the calculation considering the piston model suggests that, in this experiment, we deal with the uniform plasma piston whose structure has not manifested any instability effects. This is also proved by the correlation of experimental oscillograms current density detectors (Fig. 6a) and their calculated analogs determined in the corresponding cross sections of the channel (Fig. 6b).

Mathematical Simulation of Plasmoid Initiation in the Airflow Experiment

In the preceding experiment, an impulse discharge of a capacitor bank was used to initiate a plasmoid whose parameters were sufficient for subsequent pickup in the magnetic field and formation of a T-layer from it. However, because plasmoid parameters were not determined experimentally, it was unknown how useful the discharge energy had been spent, that is, whether one could receive a pickup with less energy expenditure.

This section describes the results of numerical simulation of a discharge process. The important factor of the experiment is the initial phase of discharge in the gas ahead of a shock wave. To model this phase, the calculation dealt with solving the problem of the shock wave input through a slot nozzle into the expansion channel from a shock tube. The solution was carried out in quasi-one-dimensional codes, and as seen in Fig. 7, it was necessary to ensure a continuous transition in numerical count through a channel section with the sharp change of a cross section. In the numerical model, transition from a subsonic mode after the reflected shock wave to a supersonic one in the section of the nozzle throat was represented as a mathematical break, where relationships for steady isentropic flow are executed.

The result of the mathematical simulation of the initiation of the shock in the nozzle is given in Fig. 8. Distributions of velocity and pressure are given for a number of successive moments of time, which enables the detection of the dynamics of the formation a shock wave deceleration in the nozzle following the start shock wave. Calculation results agree well with the experimental data, disagreement in all parameters not exceeding 10%.

Simulation of the initiation process of a plasmoid was carried out in the following way.²⁰ In rarefied air ahead of the start shock wave, when it is 90 mm from the nozzle throat (it corresponds to the conditions of the experiment), background electric conductivity σ_0 is designated. This constant value was selected about 1 S/m

Fig. 7 T-layer initiating experiment scheme in the air flow. Pulse MHD channel is switched on by the shock tube. The $P(x)$ curve shows pressure distribution at the supersonic starting stage.

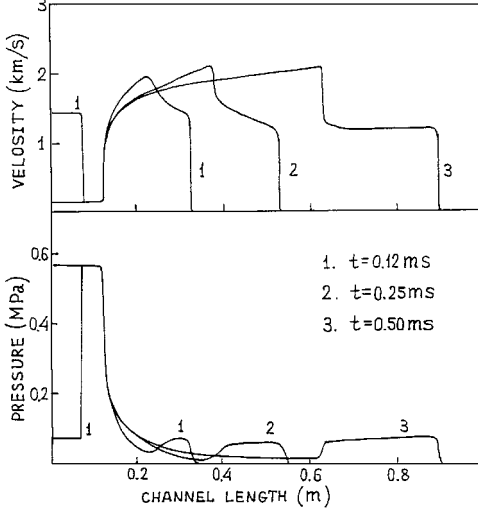
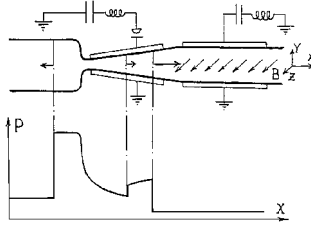


Fig. 8 The simulation result of supersonic nozzle shock starting process. Velocity and pressure distribution is given for three sequential moments.

and added to the equilibrium electric conductivity $\sigma(P, T)$, which in a developed discharge had the value $\geq 10^3$ S/m. Thus, a small increase of the conductivity did not influence the MHD interaction, but did enable the start of the discharge process of the condenser bank connected to the electrodes of the initiation section. The initial voltage across the battery $V_0 = 5 \times 10^3$ V creates a sufficient current density in the air before the shock wave to warm it up and switch on thermal ionization. This process is taking place directly ahead of a shock wave because the maximum intensity of electric field exists in the nozzle channel with divergent electrodes. Further warming with the overheating instability mechanism switched on is going on just behind the shock wave front. There is localization of the discharge in a fixed part of the airflow.

For simulation of the discharge process both in the initiation section and in the working channel, equations of MHD [Eqs. (4–6)] and equations of electric engineering circuits of initiation systems and the load in the MHD channel were simultaneously solved. Both of these circuits are capacitance, inductance, and resistance connected in series, which, according to the experiment, had the following values in calculation: For the initiation system $C_1 = 300 \mu\text{F}$, $L_1 = 0.25 \times 10^{-5}$ H, $R_1 = 5 \times 10^{-2} \Omega$, and $V_1 = 5 \times 10^3$ V. For the MHD channel load $C_2 = 5500 \mu\text{F}$, $L_2 = 3 \times 10^{-5}$ H, $R_2 = 0.5 \times 10^{-2} \Omega$, and $V_1 = 500$ V.

There was practically no special ohmic resistance in these circuits. $R_2 = 0.5 \times 10^{-2} \Omega$ is the resistance of conducting wires, and $R_1 = 5 \times 10^{-2} \Omega$ is the efficient resistance of an arc spark gap used as a key in the initiation circuit.

Equations describing the electric process of a discharge can be given as follows:

$$I(R_p + R) + L \frac{dI}{dt} + \Delta V = E + \frac{q}{C} \quad (9)$$

$$\frac{dq}{dt} = -I \quad (10)$$

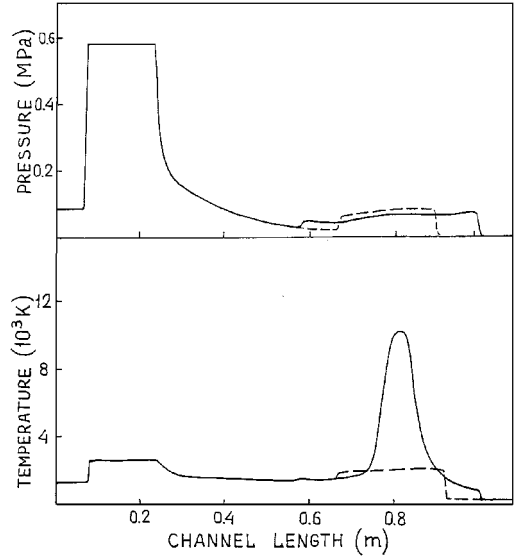


Fig. 9 Temperature and pressure distribution in the flow carrying the electric discharge. For comparison broken lines correspond to the dischargeless mode.

where

$$R_p = \left[a \int_{\delta} \frac{\sigma}{h} dx \right]^{-1}$$

is the resistance of T-layer and

$$E = R_p a \int_{\delta} (\sigma u B) dx$$

is the efficient emf acting in the plasma of the T-layer. Having solved Eqs. (9) and (10) and determined values I and q , we used them for finding the intensity of the electric field in the channel:

$$E(x) = \left(IR + L \frac{dI}{dt} + \Delta V - \frac{q}{C} \right) / h(x) \quad (11)$$

which allows us to find the distribution of current density $j = \sigma(E - uB)$. Knowing j and E , one can solve the equation system (4–6) again and find $\sigma(x)$ and $u(x)$ for the ensuing time moment.

In the problem of initiation of discharge, it was assumed that $B = 0$ and $\Delta V = 0$ (where the value ΔV is negligible as compared to the voltage across the electrodes). The calculated result of the distribution of pressure and temperature in the flow behind the front of the start shock wave is shown in Fig. 9. At the same time, corresponding distributions in the mode without a discharge are given for comparison (by the broken line). It is seen that a localized plasmod has formed with isobar distribution of pressure. The traces of gasdynamic dilatation in the form of two waves of compression are present left and right of the temperature peak.

The time dynamics of the temperature change in the discharge for four modes where σ_0 takes the values $\sigma_0^1 = 0.4$, $\sigma_0^2 = 0.5$, $\sigma_0^3 = 0.7$, and $\sigma_0^4 = 2$ S/m is given in Fig. 10. It is seen that a decrease of σ_0 results in the delay of the explosive process of heating, but the maximum temperature is attained in all of the modes practically at the same temperature $(15 \div 17) \times 10^3$ K, and after that plasma cooling begins.

The initiation system of a plasmod should convert the heat released in a discharge into internal plasma energy, that is, into its temperature, with the highest efficiency. However, in plasma parasitic processes are taking place: radiation energy losses and expansion work being done at gasdynamic dilatation of an explosively heated plasmod. To analyze these factors, the following characteristics were determined.

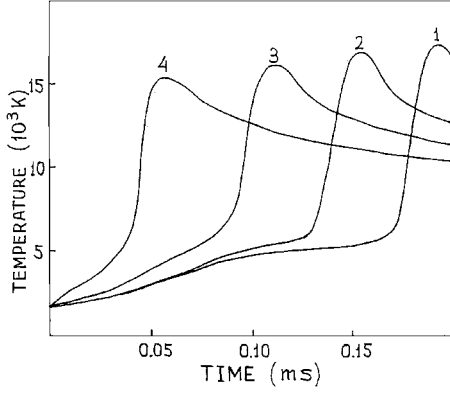


Fig. 10 The maximal temperature changing dynamics $T_{\max}(t)$ in the discharge in modes with various initial values of σ_0 : 1) $\sigma_0 = 0.4$ S/m; 2) $\sigma_0 = 0.5$ S/m; 3) $\sigma_0 = 0.7$ S/m; 4) $\sigma_0 = 2$ S/m.

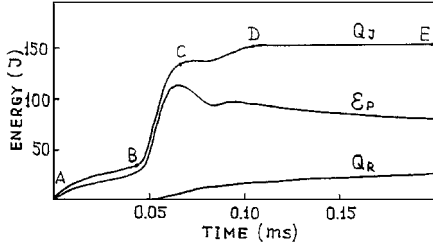


Fig. 11 Energetic discharge characteristics: Q_j -Joule dissipation energy; Q_R -radiation losses energy; ϵ_p -plasma internal energy.

Joule dissipation energy:

$$Q_j(t) = \int_{t_0}^t I^2 R_p dt$$

Radiation energy losses:

$$Q_r(t) = \int_{t_0}^t \int_{\delta} q_r A dx dt$$

Change of internal energy of a plasmoid:

$$\epsilon_p = \int_{\delta} \epsilon(t, x) \rho(t, x) A dx - \int_{\delta} \epsilon(t = 0, x) \rho(t = 0, x) A dx$$

Figure 11 shows these characteristics for the mode with $\sigma_0 = 2$ S/m. In the process of discharge one can distinguish four stages:

1) In the AB section (Fig. 11), on the curve $Q_j(t)$, slow heating in the mode similar to an isobar is proceeding. The difference between Q_j and ϵ_p is caused by the difference between c_p and c_v .

2) In the BC section (Fig. 11), the overheating instability mechanism has switched on, which resulted in a very quick warming up of plasma. The mode is similar to an isochore mode so that the curves Q_j and ϵ_p practically coincide. Cessation of the growth of Q_j and ϵ_p is due to current decrease in the oscillatory circuit in the second quarter of the first half-cycle.

3) In the CD section (Fig. 11), a quick warming up in the preceding phase has formed a pressure peak in the discharge zone. This phase is characterized by the gasdynamic expansion of the discharge zone. The process is similar to the adiabatic one; ϵ_p is decreasing because the internal energy is consumed for doing expansion work. In this phase, the plasma temperature is the highest, and it is here that the powerful radiation energy losses occur, which accounts for up to 50% of the unbalance between Q_j and ϵ_p .

4) In the DE section (Fig. 11), the energy put into the plasma is given off mainly in the first half-cycle of the discharge. In this phase, heating up has already ceased, but processes of gasdynamic expansion and radiation cooling are proceeding, though with decreasing intensities, which results in a continuous drop of ϵ_p .

Table 2 Data correlation

Parameter	Calculation	Experiment
Peak amplitude of the discharge current, kA	34	35
Current layer thickness at the nozzle output, cm	8	10
Plasmoid velocity, km/s	1.35	1.4

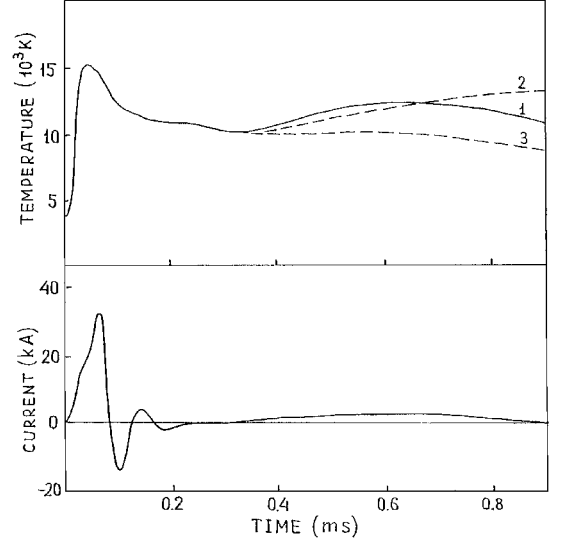


Fig. 12 T-layer forming process dynamics showed by temporal dependencies $I(t)$ and $T_{\max}(t)$. There are three modes different in the load parameters: 1) there is a charge capacitor in the load; 2) pure ohmic load, electrode voltage drop $\Delta V = 0$; 3) pure ohmic load, electrode voltage drop $\Delta V = 300$ V.

The data from the calculation and the experiment are given in Table 2; their correlation enables us to draw a conclusion on the adequacy of the mathematical model to a real process.

The created mathematical model also enabled the study of the dynamics of the process in the final stage, when the gas flow brings a plasmoid into the MHD channel. In the calculation the electrode voltage drop was designated as a constant $\Delta V = 300$ V, and the value of the magnetic field was selected according to the experiment as $B = 1$ T. The result is given in Fig. 12 in the form of relationships $I(t)$ and $T_{\max}(t)$, which reflect all stages of initiation and the working process in the MHD channel. The continuous curve for $T_{\max}(t)$ corresponds to the load circuit with a charged capacitor. The broken lines indicate the mode with pure ohmic resistance of the load (upper $\Delta V = 0$, lower $\Delta V = 300$ V). The current in the plasma, at the discharge of the load capacitor, has the peak value of 2800 A, which is somewhat lower than the experimental value ($I_{\max} = 3000$ A).

Thus, in the course of numerical simulation we were able to show the applicability of a piston model for the description of the T-layer, which gave results in accordance with the experiment, within the limits of its accuracy.

Conclusions

A new concept of the application of the MHD generator with the T-layers as a source of electric energy on a hypersonic airplane, converting kinetic energy of the air stream into electric energy, has been formulated.

The one-dimensional mathematical simulation showed that an unseeded nonuniform gas-plasma flow where plasmoids (T-layers) set up a high efficient electric conductivity at a low mass average air temperature can convert up to 30% of the kinetic energy into electric energy in the course of the MHD interaction.

An MHD generator with T-layers as an airborne generator will work efficiently at low values of magnetic field. The optimum value is close to the value $B \approx 0.3$ T, which is easily realized by a permanent magnet.

The experiment with a shock tube/MHD facility allowed us to show the method of initiation of the T-layer in a supersonic airflow. In addition, the stability of the piston structure of the plasma layer has been shown in the course of interacting with gas flow and a magnetic field. Experimental results are in good agreement with the calculation parameters of the T-layer derived from the piston model.

Mathematical simulation of the experimental process of a discharge in the airflow behind the shock wave has shown that, in the course of the initiation process of the T-layer, up to 50% of the input plasma thermal energy is lost because of gasdynamic expansion and radiation losses. The generator will be an efficient device if losses at the initiation of a T-layer do not exceed 50%.

Acknowledgment

This was made possible in part by Grant RKQ000 from the International Science Foundation.

References

- ¹Vasilyev, E. N., Ovchinnikov, V. V., and Slavin, V. S., "The Diagram of State of Stabilized Current Layer in the Channel of the MHD Generator," *Reports of Academy of Sciences of USSR Journal*, Vol. 290, No. 6, 1986, pp. 1305–1309.
- ²Fraidenraich, N., Medin, S. A., and Thring, M. W., "The Possibilities of Straited Layer MHD Generation," *Proceedings of the 2nd International Symposium on MHD Electrical Generation*, Vol. 2, 1964, pp. 781–803.
- ³Tikhonov, A. N., Samarsky, A. A., Zaklyazminsky, L. A., Volosevich, P. P., Gol'dina, D. A., Degtyarev, A. M., Kurdyumov, S. P., Popov, Yu. P., Ravinskaya, V. N., Sokolov, V. S., Favorsky, A. P., "A Non-Linear Effect of Formation of the Self-Maintained High Temperature Electrically Conducting Gas Layer in Unsteady Process of Magnetohydrodynamics," *Reports of Academy of Sciences of USSR Journal*, Vol. 173, No. 4, 1967, pp. 808–811.
- ⁴Kerkis, A. J., Sokolov, V. S., Trynkina, N. A., and Fomichev, V. P., "A Few Results of Experimental Investigation of a Current Layer," *Applied Mechanics and Technical Physics*, No. 3, 1974, pp. 31–37 (in Russian).
- ⁵Katznesol, S. S., and Slavin, V. S., "The Calculation of Plasma Flow in the Radial MHD Channel Considering Two-Dimensional Magnetic Field," *Magnetohydrodynamics*, No. 1, 1977, pp. 49–55 (in Russian).
- ⁶Derevyanko, V. A., Slavin, V. S., and Sokolov, V. S., "A MHD Generator with T-Layers," *Proceedings of the 8th International Conference on MHD Electrical Power Generation*, Nauka Pub., Moscow, Vol. 2, 1983, pp. 13–20 (in Russian).
- ⁷Slavin, V. S., "Final Results of the Theoretical Study of the Development Problems of MHD Generator with Self-Maintained Current Layers," *Magnetohydrodynamic Journal*, Vol. 2, No. 2–3, 1989, pp. 127–140.
- ⁸Bituryn, V. A., Likhachev, A. P., and Merck, W. F. H., "On the Problem of Efficiency of the MHD Generator with Space- and Time-Dependent Current Carrying Nonuniformities," *Proceedings of the 11th International Conference on MHD Electrical Power Generation*, International Academic Pub., Vol. 2, 1992, pp. 666–674.
- ⁹Wideman, J. K., Kunje, J. F., Miles, J. B., Prelas, M. A., Sschmunk, R. E., "Feasibility Analysis of an Aircraft MHD," *Proceedings of the 26th Symposium on Engineering Aspects of MHD (SEAM)*, 1988, pp. 8.2.1–12.
- ¹⁰Vasilyeva, R. V., Erofeev, A. V., Zuev, A. D., Kuranov, A. L., Lapushkina, T. A., Mirshanov, D. N., "The Experiments on MHD Energy Transformation of Supersonic Air Flow into Electricity," *Journal on Technical Physics*, Vol. 64, No. 2, 1994, pp. 49–63.
- ¹¹Slavin, V. S., Zelinsky, N. I., Lazareva, N. N., and Persianov, P. G., "Disk Closed Cycle MHD Generator with Faraday-Type Channel Working on Pure Noble Gas," *Proceedings of the 11th International Conference on MHD Electrical Power Generation*, International Academic Publishers, Vol. 4, 1992, pp. 1190–1198.
- ¹²Bozhkov, A. R., Zelinsky, N. I., and Sapozhnikov, V. A., "One-Dimensional Tables for Calculation of Thermodynamic Properties of Air," Preprint, Computing Centre, Krasnoyarsk, Russia, 1986 (in Russian).
- ¹³Sokolova, I. A., "The Coefficients of Transfer and Integrals of Collision of Air and Components," *Physical Kinetics*, Inst. Theoretical and Applied Mechanics, Novosibirsk, Russia, 1974, pp. 39–104 (in Russian).
- ¹⁴Kamenshikov, V. A., Plastinin, Yu. A., Nikolaev, V. M., Novitsky, L. A., "Radiation Properties of Gases at High Temperatures," *Mashmostroenie*, Moscow, 1971, pp. 404–437 (in Russian).
- ¹⁵Vasilyev, E. N., Slavin, V. S., and Tkachenko, P. P., "The Slip Effect of a Discharge Stabilized with the Walls of Magnetohydrodynamic Channel," *Journal of Applied Mechanics and Technical Physics*, No. 4, 1988, pp. 10–16 (in Russian).
- ¹⁶Zelinsky, N. I., and Sapozhnikov, V. A., "Correction Method for Construction of Differential Schemes of Gasdynamics Problem," *Numerical Methods of Solid Medium Mechanics*, Vol. 14, No. 3, 1983, pp. 79–87 (in Russian).
- ¹⁷Ricateau, P., and Zettwoog, P., "MHD Conversion in Inhomogeneous Flow," *Proceedings of the Symposium on Engineering Aspects of MHD (SEAM)*, Berkely, CA, 1963, pp. II.2.1–14.
- ¹⁸Derevyanko, V. A., Gavrilov, V. M., Slavin, V. S., Sokolov, V. S., Vasil'ev, E. N., "Experimental Investigations of Self-Maintained Current Layer in the MHD Channel," *Proceedings of the 9th International Conference on MHD Electrical Power Generation*, Vol. 4, 1986, pp. 1685–1694.
- ¹⁹Vasilyev, E. N., Derevyanko, V. A., and Slavin, V. S., "A Stabilized Current Layer," *High Temperature Journal*, Vol. 24, No. 5, 1986, pp. 844–851 (in Russian).
- ²⁰Bozhkov, A. R., Zelinsky, N. I., and Muschailova, S. E., "Numerical Investigation of Processes in the MHD Channel with a Current Layer," *High Temperature Journal*, Vol. 27, No. 6, 1989, pp. 1199–1205 (in Russian).